

# Bidirectional Seismic Behavior of Controlled Rocking Four-Legged Bridge Steel Truss Piers

Michael Pollino, M.ASCE<sup>1</sup>; and Michel Bruneau, F.ASCE<sup>2</sup>

**Abstract:** The behavior and design of four-legged controlled rocking bridge steel truss piers to three components of seismic excitation are presented in this paper. The controlled rocking approach for seismic protection allows a pier to uplift from its base, limiting the force demands placed on the bridge pier and deck, and can allow the structure to remain elastic during an earthquake, preventing damage toward the goal of keeping the bridge operational immediately following the earthquake. Passive energy dissipation devices [steel yielding devices (SYDs) or fluid viscous dampers (VDs)] are used at the uplifting location to control pier response. The bidirectional kinematic and hysteretic cyclic behavior of controlled rocking piers with SYDs is presented and verified with nonlinear static pushover analysis. This fundamental behavior is used to develop design equations to predict peak pier displacements, uplifting displacements, and forces (frame shear and leg axial force). Dynamic response history analyses are performed, compared with the design equations, and shown to provide reasonably accurate results for design. The use of fluid VD's in the controlled rocking system is then discussed.

**DOI:** 10.1061/(ASCE)ST.1943-541X.0000262

**CE Database subject headings:** Seismic effects; Design; Piers; Energy dissipation; Trusses.

**Author keywords:** Controlled rocking; Seismic; Behavior; Design; Bridge piers; Rocking; Passive energy dissipation.

## Introduction

As the focus on the seismic design of critical structures shifts from a methodology that aims to achieve collapse prevention and life safety (allowing damage to structural members) to one that focuses on limiting downtime (or keeping structures fully functional) following major seismic events, approaches for the seismic retrofit of existing bridges or design of new bridges that provide this increased level of performance, at a reasonable cost, are needed. Allowing the rocking of bridge piers and towers may in some instances serve this purpose. Recently, the reliance on stable rocking to provide satisfactory seismic performance has received a renewed interest: more research is being conducted on this topic and various levels of rocking response have been considered in the retrofit of large bridges. This is in part due to a growing appreciation for the ability of rocking systems to withstand seismic demands with little to no damage while providing a self-centering ability following an earthquake.

This paper discusses the bidirectional behavior and design of controlled rocking four-legged piers. Bridges supported on steel truss piers often have many two-legged piers primarily designed to support gravity loads that also resist transverse lateral loads but do not provide any significant resistance to longitudinal lateral

loads. Where four-legged piers are used, they provide support for gravity loads, transverse loads, and are the primary elements for resisting longitudinal lateral loads (together with abutments) in some instances. Expanding the controlled rocking concept developed in Pollino and Bruneau (2007) for a two-legged pier to make it applicable for the seismic resistance of four-legged piers requires a fundamental understanding of the bidirectional behavior of controlled rocking piers and the development of design equations considering ground motions in two horizontal directions in addition to the vertical direction. The controlled rocking approach for seismic resistance of bridge steel truss piers creates nonlinear elastic behavior of the pier by allowing uplifting at the base of pier legs and a restoring force provided by gravity. Energy dissipation devices installed across the uplifting location control response to within allowable limits to protect the pier. For comparison, a fixed-base pier with diagonal bracing members would behave similar to a concentrically braced frame (AISC 2005) for which, in these types of bridges, the postelastic strength and stiffness degradation of the diagonal members are known to be quite severe (Lee and Bruneau 2004), resulting in poor seismic behavior. The bidirectional behavior of controlled rocking four-legged piers is first investigated, and a method is proposed for the design of controlled rocking four-legged piers using steel yielding devices (SYDs) as the passive energy-dissipating elements. Both static and dynamic nonlinear analyses are performed to evaluate the controlled rocking response and the proposed design procedure. Finally, the use of fluid viscous damping devices is considered as the passive energy dissipation element in the controlled rocking system.

<sup>1</sup>Assistant Professor, Dept. of Civil Engineering, Case Western Reserve Univ., Cleveland, OH 44106; formerly, Simpson, Gumpertz, and Heger Inc., 41 Seyon St., Bldg. 1, Suite 500, Waltham, MA 02453 (corresponding author). E-mail: mcp70@case.edu

<sup>2</sup>Professor, Dept. of Civil, Structural and Environmental Engineering, Univ. at Buffalo, Buffalo, NY 14260. E-mail: bruneau@buffalo.edu

Note. This manuscript was submitted on March 24, 2009; approved on June 10, 2010; published online on June 15, 2010. Discussion period open until May 1, 2011; separate discussions must be submitted for individual papers. This paper is part of the *Journal of Structural Engineering*, Vol. 136, No. 12, December 1, 2010. ©ASCE, ISSN 0733-9445/2010/12-1512-1522/\$25.00.

## Previous Research and Implementation of Rocking and Self-Centering Systems

Evidence of rocking of structures has been observed following major earthquakes and used to explain how slender structures

may have been able to survive strong earthquakes (Housner 1963). The study of rocking structures possibly started with investigation of the free-vibration response of rigid rocking blocks and their response to some simple forms of dynamic loading as well as to earthquake excitations. Housner (1963) concluded that “the stability of a tall slender block subjected to earthquake motion is much greater than would be inferred from its stability against a constant horizontal force.”

From that point, analytical and experimental work has been performed to predict the response of rocking structures to earthquake motions. Many investigated the response of rigid blocks with emphasis on preventing overturning. Meek (1975) first introduced aspects of structural flexibility to the seismic response of rocking structures. Psycharis (1982) followed with an analytical study of the dynamic behavior of simplified multidegrees of freedom uplifting structures supported on flexible foundations.

Shake-table testing of rocking structures has been performed by a few researchers. Kelley and Tsztoo (1977) tested an approximately half-scale three-story steel frame that was designed with base connections to prevent horizontal movement, and mild steel torsionally yielding bars used as energy-dissipating devices at the uplifting location. Test results indicated that the rocking concept with energy-dissipating devices provided beneficial response, in terms of base shear, compared to the same frame with a fixed base (without uplift). Priestley et al. (1978) tested a simple single-degree-of-freedom (SDOF) model that was subjected to free-vibration response, sinusoidal excitations, and the 1940 N-S El Centro record. Results verified Housner’s theory on the amplitude dependent frequency assuming inelastic collisions, and the simple method developed by Priestley et al. (1978) predicted the maximum displacements with reasonable accuracy, especially for design purposes. It was noted during testing that no significant rebound occurred after impact and that large vertical accelerations were induced during impact. Toranzo et al. (2009) tested a rocking wall system for buildings that used steel flexural yielding elements that were placed at the uplifting locations to increase lateral strength and provide energy dissipation. Midorikawa et al. (2003) experimentally examined the response of a steel braced frame, allowing uplift at column bases and yielding specially designed base plates. It was found that the system effectively reduced the seismic response of building structures and that the base plates were able to provide reliable performance for the uplifting displacements while transferring shear forces. However, no studies have considered four-legged piers subjected to multidirectional earthquake excitations.

A few bridges currently exist in which rocking of the piers during earthquakes has been allowed to achieve satisfactory seismic resistance. The South Rangitikei Rail Bridge, in Mangaweka, New Zealand, has been designed and constructed in the 1970s with pier legs allowed to uplift under seismic loads (Priestley et al. 1996). The North Approach of the Lions’ Gate Bridge, in Vancouver, B.C., was seismically upgraded during the 1990s using a rocking approach for seismic resistance that implemented flexural yielding steel devices at the anchorage interface to control the response (Dowdell and Hamersley 2001). The engineers used a three-dimensional nonlinear dynamic time history model of the approach spans for prediction of maximum displacements and forces.

The benefits of allowing partial uplift of the legs of bridge piers has also been recognized and adopted for the retrofit of the Carquinez Bridge (Jones et al. 1997), the Golden Gate Bridge (Ingham et al. 1997), and the San Mateo-Hayward Bridge (Prucz et al. 1997), all in California. Note that Pier E17 of the San

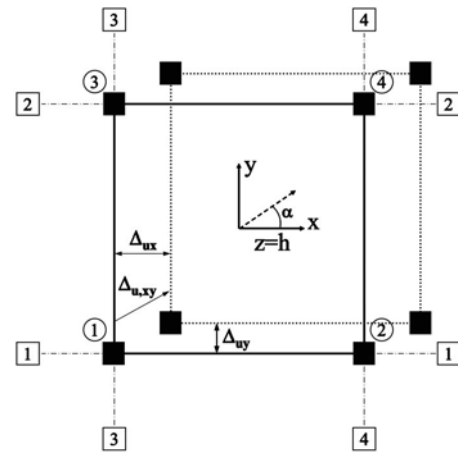


Fig. 1. Plan layout for a typical four-legged steel truss bridge pier

Francisco-Oakland Bay Bridge rocked during the Loma Prieta earthquake (Housner 1990).

Exhibiting similar behavior to rocking structures are structures in which posttensioned strands provide a significant restoring force to recenter the structure (instead of gravity alone), but such systems are beyond the scope of this paper [for bridge applications, see Mander and Cheng (1997), Palermo et al. (2005), and Marriott et al. (2006), to name a few].

### Cyclic Hysteretic Behavior of Four-Legged Pier Considering Unidirectional Motion

The plan layout of a four-legged truss pier is shown in Fig. 1 along with a coordinate system and a directional vector that lies in the  $x$ - $y$  plane at an angle  $\alpha$  from the  $x$ -axis and which will be used throughout this paper. The kinematic and hysteretic behavior of a controlled rocking four-legged pier with implemented SYD is developed here and used to establish design rules and methods.

Following the procedure used in Pollino and Bruneau (2007) to develop the cyclic hysteretic curve for a two-legged pier, the key variables for the unidirectional behavior ( $\alpha = n\pi/2$ ,  $n = 0, 1, 2, \dots$ ) of a four-legged controlled rocking pier using SYD are described in Table 1. The cyclic hysteretic curve for a four-legged pier undergoing unidirectional response can be defined similar to two-legged piers in Pollino and Bruneau (2007) with slight modifications to hysteretic variables. For a four-legged pier undergoing unidirectional motion in either of the orthogonal  $x$ - and  $y$ -directions, the cyclic hysteretic curve is shown in Fig. 2 for the relevant variables defined in Table 1. The primary difference between the unidirectional hysteretic behavior of two-legged and four-legged piers is the use of four SYDs (one at the base of each leg) and two pier frames in each direction. The use of identical devices at the base of each pier leg is recommended to ensure symmetrical behavior. The cyclic hysteretic curve defined in this manner is not path dependent beyond the second cycle (Pollino and Bruneau 2007).

Note that for four-legged piers with a SYD attached at the base of each leg,  $F_d < w_v/4$  is required to ensure recentering, where  $w_v$  = vertical tributary weight of the pier and  $F_d$  = yield force of the SYD, assuming elastoplastic behavior of the SYD. Normalizing  $F_d$  by  $w_v/4$  defines what is termed here as the local strength ratio ( $\eta_L$ )

**Table 1.** Variables Defining the Unidirectional Hysteretic Behavior of a Four-Legged Controlled Rocking Pier

Variable description	Variable definition
Base shear at point of uplift during first cycle	$P_{up1} = \frac{w_v}{2} \cdot \left(\frac{d}{h}\right)$
Pier displacement at point of uplift during first cycle	$\Delta_{up1} = \frac{P_{up1}}{k_o}$
Rocking stiffness (postuplift global stiffness)	$k_r = \left[ \frac{1}{k_o} + \frac{1}{2k_d \cdot (d/h)^2} \right]^{-1}$
Base shear at point of yielding of devices	$P_{y,uni} = \left( \frac{w_v}{2} + 2 \cdot F_d \right) \cdot \frac{d}{h}$
Pier displacement at point of device yielding during first cycle	$\Delta_{y1} = \left( \frac{w_v}{2k_o} + \frac{2F_d}{k_r} \right) \frac{d}{h}$
Base shear at point of compressive yielding of devices	$P_c = \left( \frac{w_v}{2} - 2 \cdot F_d \right) \cdot \frac{d}{h}$
Pier displacement at point of compressive yielding of devices	$\Delta_c = \Delta_u - \frac{4F_d \cdot d/h}{k_o} - 2 \cdot \Delta_{yd} \cdot \frac{h}{d}$
Base shear at point of uplift during second cycle	$P_{up2} = P_c = (1 - \eta_L) \frac{w_v}{2} \cdot \left(\frac{d}{h}\right)$
Pier displacement at point of uplift during second cycle	$\Delta_{up2} = \frac{P_{up2}}{k_o}$
Pier displacement at point of device yielding during second cycle	$\Delta_{y2} = \frac{(1 - \eta_L) \cdot \frac{w_v}{2} \cdot \frac{d}{h}}{k_o} + \frac{4F_d \cdot \frac{d}{h}}{k_r}$

$$\eta_L = \frac{F_d}{w_v/4} \quad (1)$$

## Bidirectional Kinematic and Hysteretic Pier Properties

Contrary to the above, the bidirectional hysteretic behavior of rocking piers is path dependent: as the structure moves in both directions in the horizontal plane, the changes in stiffness and sequence of yielding of the devices depend on the path of the motion undergone. It is possible for the structure to uplift and

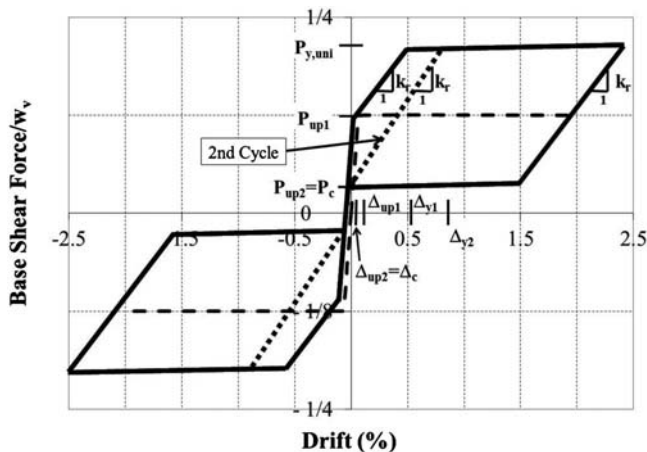


**Fig. 2.** Global cyclic unidirectional hysteretic behavior of controlled rocking system with SYD

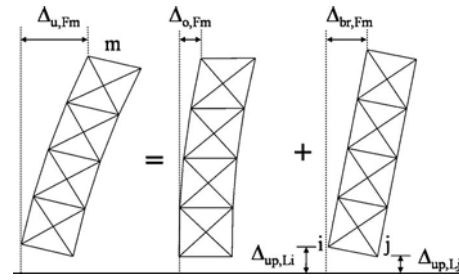


**Fig. 3.** Kinematics of controlled rocking truss pier

yield three of the devices such that it is supported on a single leg. While it is not possible to know the path of the structure for design purposes, it is important to understand the bidirectional behavior in order to predict bounds on its response in terms of displacements and forces. Assuming that the displacements caused by rotation of the pier about a vertical axis are insignificant (i.e., neglecting torsion), which can be achieved by a guiding base design for the rocking tower legs and recognizing that these piers typically have high torsional rigidity due to their in-plane cross-bracing and absence of significant mass eccentricity (the theory presented here would have to be expanded in those rare instances when this is not the case), using the notation illustrated in Fig. 1, the top of frames along Lines 1-1 and 2-2 experiences the same horizontal displacements while frames along Lines 3-3 and 4-4 experience the same displacements. The displacement of the top of arbitrary frame  $m$  ( $\Delta_{u,Fm}$ ) is the sum of deformations due to flexibility of frame's structural members ( $\Delta_{o,Fm}$ ) and rigid body rotation at the base of the frame ( $\Delta_{br,Fm}$ ) (see Fig. 3) such that

$$\Delta_{u,Fm} = \Delta_{o,Fm} + \Delta_{br,Fm} \quad (2)$$

where the displacement due to deformation of the frame's structural members ( $\Delta_{o,Fm}$ ) can be determined using methods of structural analysis. The displacement due to rigid body rotation of frame  $m$  ( $\Delta_{br,Fm}$ ) is related to the uplifting displacement of the frame ( $\Delta_{up,Fm}$ ), which is defined as the difference of the uplifting displacement of the two legs ( $i$  and  $j$ ) of the frame such that

$$\Delta_{br,Fm} = \Delta_{up,Fm} \cdot h/d = (\Delta_{up,Li} - \Delta_{up,Lj}) \cdot h/d \quad (3)$$

where  $\Delta_{up,Li}$  and  $\Delta_{up,Lj}$  = larger and smaller uplifting displacements of the frame legs, respectively (for a pier height and width of  $h$  and  $d$ , respectively), as shown in Fig. 3.

Since each pier leg "belongs" to two frames (one in each of the  $x$ - and  $y$ -directions), the uplifting displacement of any given pier leg is dependent on the pier lateral displacement in the  $x$ - and  $y$ -directions. For example, considering a global displacement in the  $+x$ - and  $y$ -directions such that Pier Leg 4 remains in contact with its support, the uplifting displacement of Pier Leg 1 (see Fig. 1 for pier leg numbers) can be determined by summing the uplifting displacements of Frames 4 and 1 or Frames 2 and 3 (where frame  $m$  = frame located along Line  $m$ - $m$  in Fig. 1). Using Frames 4 and 1, the uplifting displacement of Pier Leg 1 is determined using Eqs. (2) and (3), where  $i=1$ ,  $j=2$ , and  $m=1$  such that

$$\Delta_{up,L1} = \Delta_{up,L2} + (\Delta_{u,F1} - F_{F1}/k_f) \cdot d/h \quad (4)$$

where  $\Delta_{up,L2}$  can be determined using Eqs. (2) and (3) with  $i=2$ ,  $j=4$ , and  $m=4$  such that

$$\Delta_{up,L2} = \Delta_{up,L4} + (\Delta_{u,F4} - F_{F4}/k_f) \cdot d/h \quad (5)$$

where  $F_{F1}$  and  $F_{F4}$ =horizontal shears applied to Frames 1 and 4, respectively, and  $k_f$ =stiffness of a single frame. If the top of pier displacements are in the positive  $x$ - and  $y$ -directions, and ignoring torsion as indicated earlier, then  $\Delta_{u,F1}=\Delta_{u,F2}=\Delta_{u,x}$ ,  $\Delta_{u,F3}=\Delta_{u,F4}=\Delta_{u,y}$ , and  $\Delta_{up,L4}=0$ . The corresponding uplifting displacement of Legs 1, 2, and 3, respectively, is given by

$$\Delta_{up,L1} = \left( \Delta_{u,x} + \Delta_{u,y} - \frac{F_{F1} + F_{F4}}{k_f} \right) \cdot \frac{d}{h} \quad (6)$$

$$\Delta_{up,L2} = (\Delta_{u,y} - F_{F4}/k_f) \cdot d/h \quad (7)$$

$$\Delta_{up,L3} = (\Delta_{u,x} - F_{F2}/k_f) \cdot d/h \quad (8)$$

If the hysteretic path to reach  $\Delta_{u,x}$  and  $\Delta_{u,y}$  results in the formation of the pier's plastic mechanism defined as any pier displacement resulting in yield of three SYDs, the pier static free-body diagram shown in Fig. 3(a) is obtained. From that diagram, it is possible to separate each frame from the pier and draw free-body diagrams of each frame, as shown in Fig. 3(b) (note that columns from adjacent frames are shown twice). Through the equilibrium of forces, the horizontal shear force to Frames 1 and 3 is

$$F_{F1,3} = (w_v/8 + 1/2 \cdot F_d) \cdot d/h \quad (9)$$

and the shear force applied to Frames 2 and 4 is

$$F_{F2,4} = (3w_v/8 + 3/2F_d) \cdot d/h \quad (10)$$

Note the larger shear force on the frames attached to the pier leg that remains in contact with its support (Frames 2 and 4 for the motion considered).

Considering the special case of a continuous linear horizontal displacement path in the  $\alpha$ -direction, the bidirectional yield displacement ( $\Delta_{y,xy}$ ) is defined as the vectorial displacement at the top of the pier in the  $x$ - $y$  plane when the last device yields such that

$$\Delta_{y,xy} = \sqrt{\Delta_{y,x}^2 + \Delta_{y,y}^2} \quad (11)$$

where  $\Delta_{y,x}$  and  $\Delta_{y,y}$ = $x$ - and  $y$ -direction displacements when the yield mechanism forms.

Depending on the value of  $\alpha$ , the pier is displacing more in either the  $x$ - or  $y$ -direction (or the same if  $\alpha=n\pi/4$  rad, where  $n=1,3,5,\dots$ ) and controls the sequence of device yielding. For example, if the pier is assumed to travel in a direct path from zero pier displacements to  $\Delta_{u,x}$  and  $\Delta_{u,y}$  ( $\Delta_{u,y}=\Delta_{u,x} \tan \alpha$ ,  $0 \text{ rad} < \alpha < \pi/4$  rad) then Device 1 will yield first, followed by Device 3 and then Device 2. When  $\alpha=\pi/4$  rad, Device 1 yields first then Devices 2 and 3 yield simultaneously. When  $\alpha=0, \pi/2, \pi$ , and  $3\pi/2$  rad, only two of the devices yield and they will yield simultaneously (unidirectional response).

The pier displacement, in the smaller displacement component direction, when the third device yields ( $\Delta_{y,sc}$ ) can be determined from the kinematic frame behavior defined by Eq. (2) such that

$$\Delta_{y,sc} = \Delta_o + \Delta_{br} = F_F/k_f + \Delta_{up,Li} \cdot h/d \quad (12)$$

where  $F_F$ =frame shear force with leg in contact with support [Eq. (10)] and  $\Delta_{up,Li}$  is equal to the uplifting displacement at yield of the steel device considering second cycle properties ( $2\Delta_{yd}$ ). Finally, using Eq. (11), the bidirectional yield displacement ( $\Delta_{y,xy}$ ) is defined as

**Table 2.** Results of Nonlinear, Static Pushover Analysis and Values from Developed Kinematic/Hysteretic Properties

	Eq. #	Value	Analysis result
$\Delta_{up,L1}$	(6)	193	193
$\Delta_{up,L2}$	(7)	49.0	48.0
$\Delta_{up,L3}$	(8)	137	136
$F_{F1}$	(9)	81.0	81.0
$F_{F3}$	(9)	81.0	81.0
$F_{F2}$	(10)	243	243
$F_{F4}$	(10)	243	243
$\Delta_{y,xy}$	(11)	231	239.6
$\Delta_{y,sc}$	(12)	85.7	88.9
$P_{y,xy}$	(14)	459	459

Note: All units in kN and mm.

$$\Delta_{y,xy} = \Delta_{y,sc} \sqrt{1 + 1/\tan^2(\alpha)} \quad (-\pi/4 < \alpha < \pi/4, 3\pi/4 < \alpha < 5\pi/4)$$

$$\Delta_{y,xy} = \Delta_{y,sc} \sqrt{1 + \tan^2(\alpha)} \quad (\pi/4 < \alpha < 3\pi/4, 5\pi/4 < \alpha < 7\pi/4) \quad (13)$$

Once the pier has reached the displacement defined in Eq. (13) to form the bidirectional yield mechanism, the maximum static forces can be determined from the equilibrium diagrams for the pier shown in Fig. 3. It can be shown that the maximum shear force in each direction is equal to the unidirectional yield force,  $P_{y,uni}$  (see Table 1); thus,  $F_x=F_y=P_{y,uni}$  and the bidirectional yield force is

$$P_{y,xy} = \sqrt{F_x^2 + F_y^2} = \sqrt{2}P_{y,uni} \quad (\alpha \neq n\pi/2 \text{ rad}, n=0,1,2,\dots) \quad (14)$$

## Nonlinear Static Pushover Analysis for Verification of Static Kinematic/Hysteretic Behavior

Nonlinear static pushover analysis is used to verify and illustrate the analytical expressions defined above. A representative pier with aspect ratio  $h/d=4$  ( $h=29.26$  m,  $w_v=1,730$  kN,  $k_o=12.5$  kN/mm,  $k_f=6.25$  kN/mm) and SYD ( $\eta_L=0.50$ ,  $k_d=36.9$  kN/mm) is considered here. An elastoplastic model is used for the SYD for comparison with the expressions derived above.

This example considers a progressively increasing displacement applied in the  $\alpha$ -direction such that  $\alpha=\tan^{-1}(0.4/1.0)=21.8^\circ$ . This direction of  $\alpha$  was chosen to achieve a maximum displacement following the 100-40% directional combination rule that is often applied for the seismic design of bridges (ATC/MCEER 2004). The pier is pushed until a displacement equivalent to 2.0% drift is reached in one of the principal directions. The pushover curve is defined as the resulting shear in the  $\alpha$ -direction ( $F_{xy}$ ) versus the displacement along the  $\alpha$ -direction ( $\Delta_{xy}$ ). The resulting pushover curve is shown in Fig. 5 along with the unidirectional pushover curve for comparison. The pushover curve changes slope 6 times as each of the three legs uplifts from the foundation and each of the steel devices yields. Results of the pushover analysis are compared in Table 2 with the response parameters derived earlier. The maximum developed base shear is equal to the pier's plastic capacity defined by Eq. (14). As can be seen from the table, the derived values of uplifting displacements and frame forces agree with the results of nonlinear pushover analysis.

## Simplified Analysis Method Considering Bidirectional Horizontal Input

To predict maximum pier displacements for design, the capacity spectrum analysis method (ATC/MCEER 2004) is used which characterizes an MDOF nonlinear system by a linear-viscous SDOF system. The simplification to the SDOF system is done by developing the structural capacity (pushover) curve of the multiple-degree-of-freedom (MDOF) system, in a particular direction, using a loading profile corresponding to the first mode of vibration (assuming this to be the dominant mode). The hysteretic energy dissipated ( $W_d$ ) is converted to an assumed equivalent amount of viscous damping per cycle by

$$\xi_{\text{eff}} = \xi_o + \xi_{\text{PED}} \quad (15)$$

where  $\xi_o$ =inherent structural damping (assumed to be 2%) and  $\xi_{\text{PED}}$ =damping provided by passive energy dissipation devices during rocking response. Note that no hysteretic energy dissipation is considered within the structure since it is designed to remain elastic. Factors for reducing the spectrum for the effective damping ( $\xi_{\text{eff}}$ ) from Eq. (15) are given in FEMA 450 (FEMA 2004). Another source of energy loss occurs during rocking response as the pier impacts the foundation and stress waves propagate away from the pier (radiation damping). The energy loss during each impact has been examined by Housner (1963); however, the amount of energy dissipated by this mechanism is small compared to the energy dissipation devices and is therefore conservatively ignored in this study.

Questions arise using this simplified analysis method for bidirectional horizontal response, such as what path to consider in the development of the structural capacity curves and what should be the corresponding demand curves. Due to the path dependency of the hysteretic behavior, the spectral capacity curve can vary for any path with  $\alpha=0$  to  $\alpha=45^\circ$ . The case of  $\alpha=0$  (unidirectional behavior in the  $x$ - or  $y$ -direction) provides a lower bound on the structural force capacity ( $P_{y,\text{uni}}$ ) and on the energy dissipated per cycle since only two of the SYDs are activated. The path with  $\alpha=45^\circ$  provides an upper bound on the structural force capacity [ $P_{y,\text{xy}}$  of Eq. (14)] and energy dissipated per cycle since all three devices are activated at the smallest displacements compared to other paths. Therefore, unidirectional controlled rocking behavior should be used to determine an upper bound on the maximum pier displacements. The corresponding demand curve for unidirectional response can be derived from the design spectrum in one of the principal pier directions.

The hysteretic damping of the controlled rocking system with SYD ( $\xi_{\text{PED}}=\xi_{\text{SYD}}$ ) is equal to

$$\xi_{\text{SYD}} = \frac{\eta_L}{1 + \eta_L} \cdot \frac{2}{\pi} \cdot \left(1 - \frac{1}{\mu_{G2}}\right) \quad (16)$$

where  $\mu_{G2}$ =displacement ductility ratio considering second cycle properties such that

$$\mu_{G2} = \Delta_u / \Delta_{y2} \quad (17)$$

where  $\Delta_u$ =maximum unidirectional pier displacement and  $\Delta_{y2}$ =pier yield displacement for four-legged piers considering second cycle properties (Table 1).

## Design Applications

The design of a controlled rocking pier for seismic design (or retrofit) requires limiting pier displacements and demands to the device while capacity design principles are applied to the pier and superstructure. The design process for two-legged piers controlled with SYD has been illustrated in detail in Pollino and Bruneau (2007). Here, those concepts are expanded upon to discuss the key design constraints to achieve the performance objectives for controlled rocking four-legged piers using SYD and, in a later section, with fluid viscous dampers (VDs).

### Pier Displacements

Limits on the pier displacements may be set to ensure pier stability or to prevent excessive movement of the bridge deck at abutments or other piers. For instance, longitudinal bridge deck movement must be limited to prevent potential unseating of spans where it is connected with roller supports for thermal expansion. Maximum displacements of a controlled rocking pier can be predicted using the simplified analysis method discussed previously (an iterative process for design). The primary system parameters that can be most easily tailored to control response are the SYD strength and stiffness.

### Uplifting Displacements

The design of the SYD requires limiting the pier leg uplifting displacements such that the devices behave in a stable, predictable manner during the design level of excitation (per specifications, manufacturer's recommendations or experimentally supported consensus), depending on the type of SYD used. The maximum uplifting displacement under bidirectional response is calculated using Eq. (6) and a 100-40 directional combination rule applied such that

$$\Delta_{\text{up},100-40} = \left[ \max \left( \begin{array}{l} 1.0\Delta_{u,x} + 0.40\Delta_{u,y} \\ 0.40\Delta_{u,x} + 1.0\Delta_{u,y} \end{array} \right) - \left( \frac{F_{F1} + F_{F4}}{k_f} \right) \right] \cdot \frac{d}{h} \quad (18)$$

### Maximum Pier Forces

Maximum pier forces developed during rocking response need to be predicted conservatively, such that the pier can remain elastic during a seismic event (capacity protection), and with reasonable accuracy for an economical design. For the case of four-legged piers, the structure needs to be designed for its response under three components of earthquake excitation. If the controlled rocking pier is designed for at least a global displacement ductility ( $\mu_{G2}$ ) of 2.5 in a single direction, then the bidirectional yield mechanism is expected to form, resulting in static forces, as shown in the free-body diagram in Fig. 4, regardless of whether the 100-40, 40-100, or 40-40 combination of the two horizontal demands is used.

The effect of the vertical excitation is included by determining the design vertical spectral acceleration value at the vertical period of the pier,  $T_L$ . Including the dynamic forces caused during impact and uplift along with the effects of vertical excitation, the free-body diagram of each pier frame is shown in Fig. 5. Using these free-body diagrams, forces in critical members, connec-

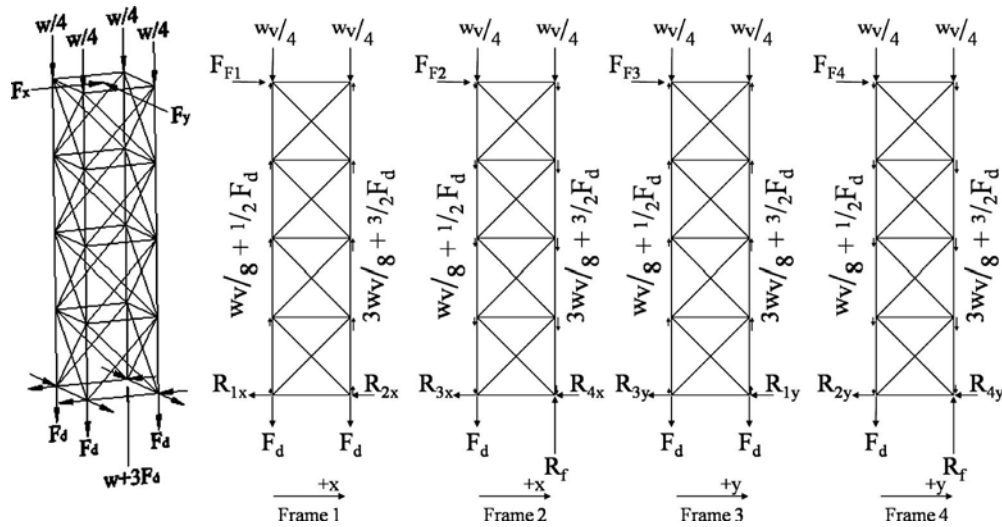


Fig. 4. Free-body diagrams of frames at formation of bidirectional plastic mechanism

tions, and other components can be determined by applying appropriate combination rules to these forces (since the forces shown are the maxima of each effect).

### Maximum Frame Shear

The maximum frame shear ( $P_{uF}$ ) includes forces from the uplift of the pier and yielding of the devices times the dynamic amplification factor during uplift ( $R_{dv}$ , derived in Pollino and Bruneau 2008) to account for increased dynamic response due to the vertical shear mode of the pier and the effect of vertical excitation. Application of the 100-40 directional combination rule to the two horizontal components of motion results in development of the bidirectional yield mechanism for  $\mu_{G2} > 2.5$ . However, when the third (vertical) component is included in the combination rule, the dynamic effect resulting during uplifting ( $R_{dv}$ ) is combined with the vertical excitation using the combination rule due to their nonsimultaneity, and the design frame shear force is taken as

$$P_{uF,100-40} = \max \left[ \begin{array}{l} P_{uF,st} + 1.0 \cdot P_{uF,st} \cdot (R_{dv} - 1) + 0.40 \left( \frac{3}{8} m_v S_{av} \frac{d}{h} \right) \\ P_{uF,st} + 0.40 \cdot P_{uF,st} \cdot (R_{dv} - 1) + 1.0 \left( \frac{3}{8} m_v S_{av} \frac{d}{h} \right) \end{array} \right] \quad (19)$$

where  $P_{uF,st}$  = Eq. (10).

### Maximum Pier Leg Axial Force

The maximum developed axial force in a pier leg ( $P_{uL}$ ) can be determined by equating vertical equilibrium from Fig. 6. The pier leg axial force includes the force effects caused by the impact of the pier leg with the foundation and increased dynamic effects that occur during pier uplifting. Considering that two pier diagonals connect to the base of the compressed pier leg, such that their load is applied directly into the support, the maximum load on the pier leg is less than the support reaction.

The pier leg axial force includes five components resulting from uplifting and yielding of devices ( $P_{uL,st}$ ), vertical excitation ( $F_{ve}$ ), and dynamic force effects during pier rocking ( $F_{vo}$ ,  $F_w$ ,  $F_{up}$ ) such that

$$P_{uL,100-40} = \max \left( \begin{array}{l} P_{uL,st} + 0.40 F_{ve} + 1.0 \sqrt{F_{vo}^2 + F_w^2 + F_{up}^2} \\ P_{uL,st} + 1.0 F_{ve} + 0.40 \sqrt{F_{vo}^2 + F_w^2 + F_{up}^2} \end{array} \right) \quad (20)$$

The first term,  $P_{uL,st}$ , is the axial force generated statically in the pier leg as a result of development of the bidirectional yield mechanism and is equal to

$$P_{uL,st} = (3w_v/4 + 3F_d) \cdot (1 - d/2h) + w_v/4 \quad (21)$$

The static component of the pier leg axial force ( $P_{uL,st}$ ) is present in all combinations. The second term is the pier leg force resulting from vertical excitation,  $F_{ve}$ , and is

$$F_{ve} = 1/4 m_v S_{av} + 3/4 m_v S_{av} \cdot (1 - d/2h) \quad (22)$$

The third term ( $F_{vo}$ ) results from the initial impacting of the pier leg after it has uplifted and is returning to its support with an impact velocity  $v_o$  and is equal to

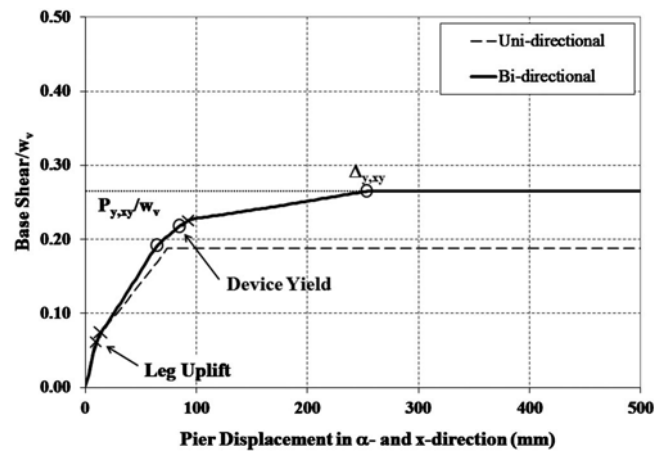


Fig. 5. Bidirectional and unidirectional pushover curves (second cycle properties)

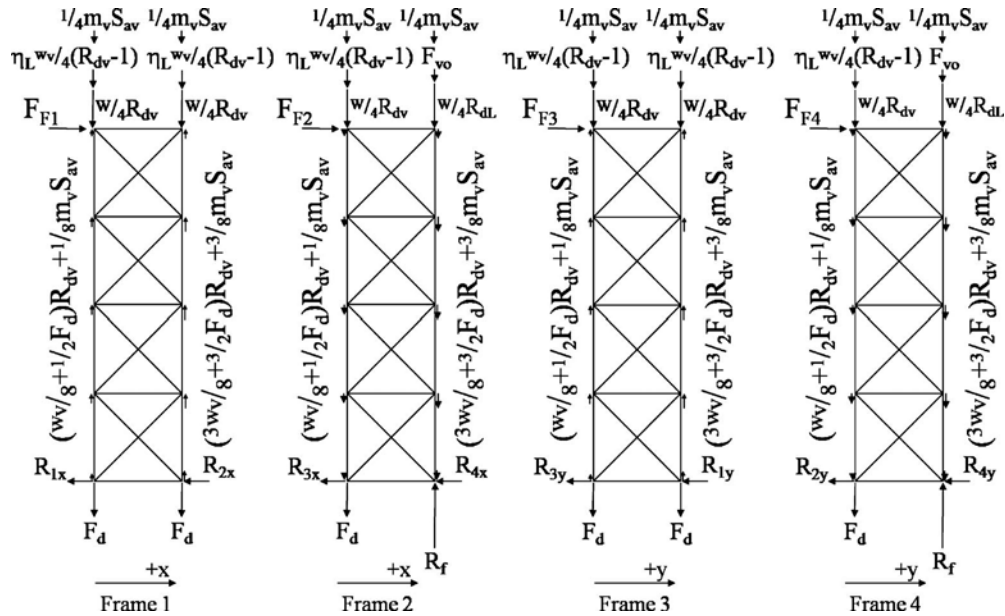


Fig. 6. Free-body diagrams of frames including forces due to dynamic effects

$$F_{vo} = v_o \cdot \sqrt{m_v k_L / 4} \quad (23)$$

The fourth term ( $F_w$ ) is the dynamic effect of the weight tributary to a single pier leg being suddenly applied as the leg returns to the support and is equal to

$$F_w = w_v / 4 \cdot (R_{dL} - 1) \quad (24)$$

The fifth term ( $F_{up}$ ) is the dynamic effect of the remaining pier tributary weight and devices' forces sudden transfer to the compressed pier leg during uplift and is equal to

$$F_{up} = (3w_v / 4 + 3F_d) \cdot (R_{dv} - 1) \cdot (1 - d / 2h) \quad (25)$$

Finally, the second term (resulting from vertical excitation,  $F_{ve}$ ) is combined using a 100-40 directional combination rule with square-root-sum-squares (SRSS) combination of horizontal modal responses described in terms 3, 4, and 5.

The impact velocity of the pier leg,  $v_o$ , can be determined using the energy balance approach developed in Pollino and Bruneau (2008) where energy is equated at the point of maximum deformation and just before the point of leg impact with the support with the nonconservative work done by the energy dissipation devices included between these two points and is equal to

$$v_{oSYD} = \sqrt{g \left( \frac{1}{\frac{1}{4} \left( \frac{h}{d} \right)^2 + 1/2} \right) \cdot \left[ \frac{w_v \eta_L^2 - 1}{2} \left( \frac{d}{h} \right)^2 + \dots \right]} \quad (26)$$

However, under bidirectional response, the impact velocity depends on the pier's motion in two horizontal directions ( $v_{oSYD,x}$ ,  $v_{oSYD,y}$ ) such that the total impact velocity,  $v_{oSYD}$ , is equal to

$$v_{oSYD} = v_{oSYD,x} + v_{oSYD,y} \quad (27)$$

and should be calculated using the directional combination rule. Pier legs may need to be reinforced to prevent their buckling

under these forces, but to a lesser extent than would be required in legs of fixed-based piers under bidirectional seismically induced overturning moments that create large uplift and compression forces in the pier legs.

### Comparison between Design Predictions and Dynamic Analysis

A set of dynamic time history analyses is conducted to evaluate the bidirectional behavior and design equations developed. The pier and energy-dissipating device properties are the same as those presented in the nonlinear pushover analysis example ( $h/d=4$ ,  $w_v=1,730$  kN,  $k_o=12.5$  kN/mm,  $\eta_L=0.50$ ,  $k_d=36.9$  kN/mm). A horizontal demand spectrum is considered with  $S_s=1.95$  g,  $S_1=0.87$  g,  $T_s=0.45$  s, and a shape as defined in ATC/MCEER (2004). The vertical spectrum is determined by decreasing the characteristic period of the horizontal spectrum ( $T_s$ ) by 1.55 and reducing the amplitude of the horizontal spectrum by 1.25. Both the horizontal and vertical design spectrums are shown in Fig. 7.

### Ground Motions

Spectra compatible ground acceleration time histories were used for the base excitation of the analytical model and were generated using the Target Acceleration Spectra Compatible Time Histories (TARSCHTS) software developed by the Engineering Seismology Laboratory at the University at Buffalo ([http://civil.eng.buffalo.edu/users\\_ntwk/index.htm](http://civil.eng.buffalo.edu/users_ntwk/index.htm)). Seven synthetic ground motions were generated for each direction ( $x$ ,  $y$ , and  $z$ ) matching the target design spectrum, as shown in Fig. 7.

### Design Response Predictions

The maximum pier displacement in one of the primary directions is predicted using the simplified analysis procedure considering unidirectional pier properties and determined to be equal to 443 mm, resulting in a total bidirectional displacement (using 100-40

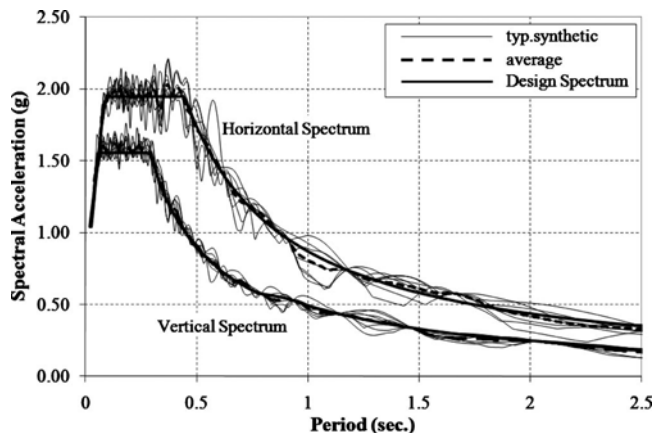


Fig. 7. Horizontal and vertical spectra

directional combination rule) of 478 mm. The maximum uplifting displacement can then be calculated from Eqs. (18), (9), and (10) and is equal to 143 mm. The dynamic amplification factors ( $R_{db}$  and  $R_{dl}$ ) are equal to 1.84 and 1.97, respectively, for the case considered. The vertical spectral acceleration value from Fig. 7, at the vertical period of the pier ( $=0.12$  s), is equal to 1.56 g. The maximum frame shear, from Eq. (19), is equal to 548 kN and the maximum pier leg axial force is determined from Eq. (20) and is equal to 4,290 kN.

### Analytical Model

The dynamic response of the structure was predicted using the program SAP2000 (Wilson 2000). The model mass is lumped in a single node at the geometric center of the top of the pier and constrained to move as a rigid diaphragm with the nodes at the top of the pier legs. The pier's structural members are modeled with elastic frame elements. Compression-only gap elements were attached to the base of the legs in the vertical and two horizontal directions to simulate a base connection that relied on bearing to resist forces in these three directions. The gap elements provided no resistance to movement vertically upward at the base of the leg or horizontally toward the inside of the pier (directions that would otherwise apply tension to the elements). The SYDs were modeled using the plasticity property of Wen (1976) that is defined by the elastic stiffness ( $k_d=36.9$  kN/mm), yield force ( $F_d=216$  kN), postyield stiffness ratio, and a parameter that controls the smoothing of the transition to yield. The postelastic stiffness was assumed to be 2% of its elastic value and the yielding parameter was set equal to 2.

Rayleigh damping was used with 2% of critical damping assigned to periods of 2.5 and 0.05 s. The upper limit of 2.5 s was chosen to limit the influence of the mass proportional damping term on the structure after it has uplifted from its base and the period of the rocking structure exceeds significantly the fixed-base period (0.74 s). The lower limit was chosen such that the important higher modes of vibration were not overdamped. No attempt was made to explicitly include radiation damping in the model; however, as noted previously, this is not expected to significantly influence response.

### Results and Discussion of Dynamic Analysis

The results of the seven time history analyses are shown in Fig. 8, as data points, along with the mean (large solid horizontal bar),

mean+ $\sigma$ , and mean- $\sigma$  response (smaller horizontal bars connected to the mean bar) of all results. Also, a solid diagonal line on each plot divides the range of conservative and unconservative predictions of response ( $y=x$ ). Both unidirectional and bidirectional pier displacements ( $\Delta_{u,x}$ ,  $\Delta_{u,y}$ , and  $\Delta_{u,xy}$ ) are shown in Fig. 7(a) since the simplified methods of analysis predict each of these quantities. The maxima of the uplifting displacement of the four pier legs, frame shear force of the four pier frames, and axial force of the four pier legs are presented in Figs. 8(b-d), respectively.

The mean predicted unidirectional displacement values in the  $x$ -direction are conservative by approximately 12% while  $y$ -direction displacements are underpredicted by approximately 2%. However, the bidirectional displacement prediction is slightly unconservative ( $\sim 8\%$  difference) using the 100-40 directional combination rule. The uplifting displacement results deviate from the predicted response by approximately the same percentage as the bidirectional displacement,  $\Delta_{u,xy}$  ( $\sim 9\%$ ), as would be expected since the uplifting displacement is primarily dependent on prediction of the maximum bidirectional pier displacement and uses the 100-40 combination rule. The maximum frame shear force and pier leg axial forces are predicted more conservatively (14 and 16% differences, respectively).

### Use of Fluid VD's in Controlled Rocking System

The use of fluid VD's as the passive energy dissipation device fundamentally changes the behavior of the controlled rocking system with SYD, but many of the concepts presented remain applicable. The use of viscous damping devices allows self-centering of the system regardless of the damper properties used. Inclusion of VD's to a controlled rocking pier will influence the cyclic hysteretic curve (considering dynamic response) and the amount of energy dissipation of the system. Such devices generate a force response dependent on the relative velocity across its two ends (Constantinou et al. 1998) such that

$$F_{VD} = c \operatorname{sgn}(v_d) \cdot |v_d|^{\alpha_d} \quad (28)$$

where  $c$ =damping coefficient;  $\alpha_d$ =damping exponent;  $v_d$ =relative velocity across the damper; and  $\operatorname{sgn}$ =sign function. The global hysteretic behavior of a controlled rocking system with VD [ $c=39.8$  kN(s/mm) $^\alpha$ ,  $\alpha_d=0.50$ ] is shown in Fig. 9 (not including higher modes of response).

### Energy Dissipation and Use of Simplified Analysis Method

The work done by the VD's in a quarter cycle of unidirectional controlled rocking motion (point of maximum displacement and back to the support,  $W_{1-2,VD}$ ), assuming sinusoidal motion, is

$$W_{1-2,VD} = 1/2 \cdot (2 \cdot \pi / T_{sec})^{(\alpha_d)} c \cdot \lambda \cdot \Delta_{upL}^{(\alpha_d+1)} \quad (29)$$

where  $\lambda$ =parameter that is equal to  $\pi$  when  $\alpha_d=1.0$  (linear VD) and equal to 3.496 when  $\alpha_d=0.50$ . The secant period of vibration,  $T_{sec}$ , is defined by

$$T_{sec} = 2 \cdot \pi \cdot \sqrt{m \cdot \Delta_u / P_{y,uni}} \quad (30)$$

The equivalent viscous damping provided per cycle of motion by the VD's is equal to

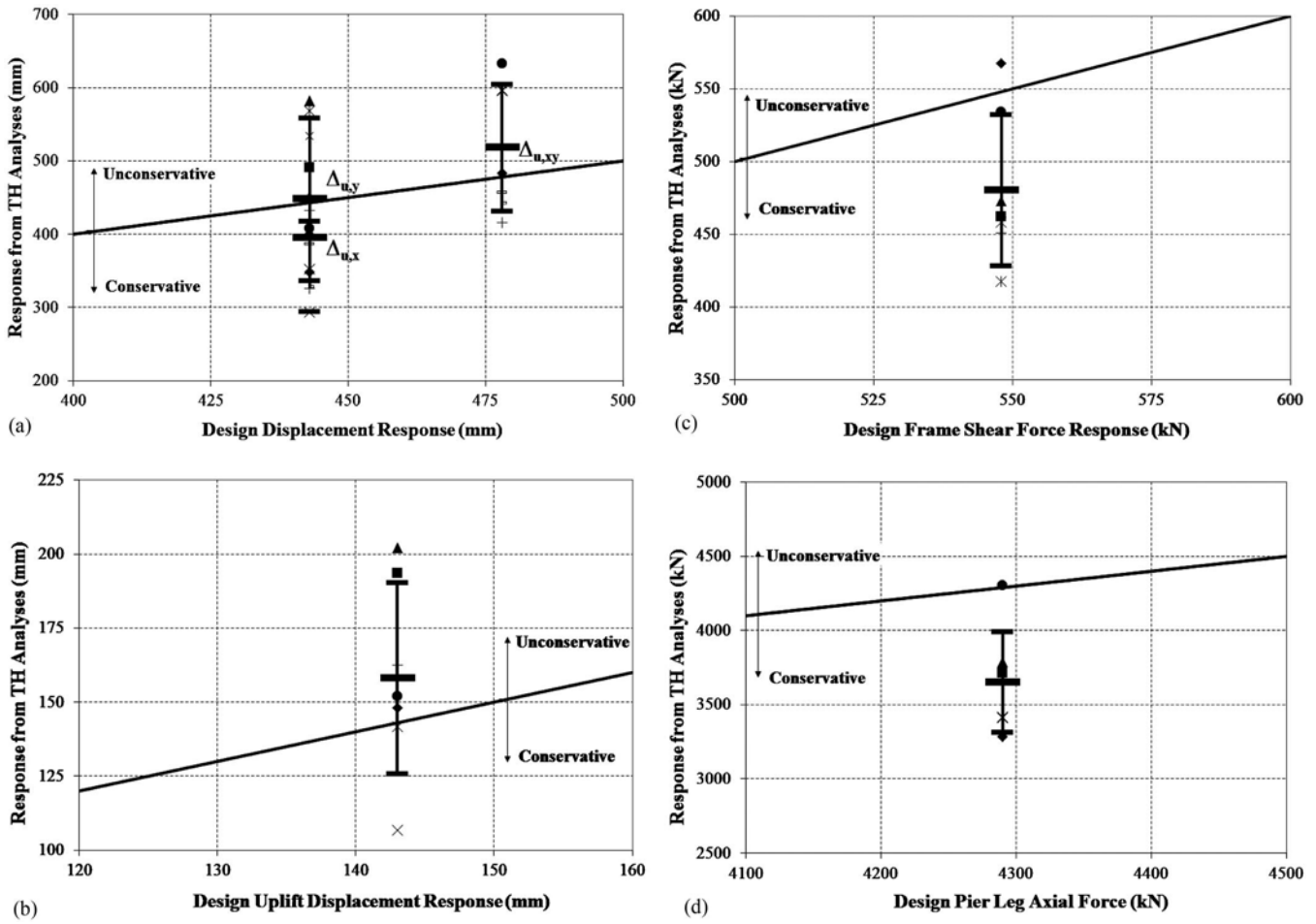


**Fig. 8.** Results of dynamic analyses and design response values: (a) maximum pier displacements;  $x$ -,  $y$ -, and  $xy$ -directions; (b) maximum uplifting displacements; (c) maximum frame shear; and (d) maximum pier leg axial force

$$\xi_{\text{eff}} = \xi_o + \xi_{VD} = \xi_o + W_{1-2,VD} / \pi \cdot W_k \quad (31)$$

where  $W_k$ =stored strain energy in the system at the maximum displacement ( $\Delta_u$ ) and is taken as

$$W_k = 1/2 \cdot P_{y,\text{uni}} \cdot \Delta_u \quad (32)$$

where  $P_{y,\text{uni}}$ =unidirectional system yield force given in Table 1 with  $F_d=0$  for VDs. The capacity spectrum method of analysis can be used to predict maximum pier displacements with the effective damping defined by Eq. (31) and structural capacity curve of a free-rocking pier.

### Peak VD Force during Controlled Rocking Response

The peak damper force is a function of the maximum velocity at the uplifting location which can be determined using an energy balance approach similar to that done for SYD [Eq. (26)] where the work done by the SYD is replaced by that done by the VD ( $W_{1-2,VD}$ ) and is equal to

$$v_{o,VD} = \sqrt{\frac{2}{m_v[(h/d)^2 + 1/2]}} \cdot \left( \Delta_{\text{up}L} \frac{w_v}{2} - W_{1-2,VD} \right) \quad (33)$$

### Design Applications with VDs

The design process of a controlled rocking pier with fluid VDs implemented is similar to that for SYD, with a few differences that pertain to the force output and energy dissipated by the devices. To limit pier forces, the damper needs to be designed to control its output force by limiting the uplifting velocity [the use

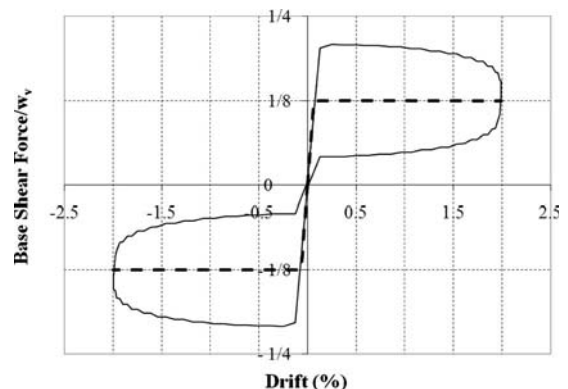


**Fig. 9.** Global cyclic hysteretic behavior of controlled rocking system with fluid VDs

of nonlinear VD's ( $\alpha < 1$ ) is also useful for this purpose]. The pier displacements can be controlled by selection of appropriate damping coefficient ( $c$ ) and damping exponent ( $\alpha_d$ ). The uplift displacement can be determined using Eq. (18) with  $F_d=0$  (since at peak pier displacement the pier has zero velocity and the damper will have no force output). The peak frame shear force can be calculated by Eq. (19) and the peak pier leg axial force by Eq. (20), both with  $F_d=F_{vd}$  [Eq. (28)] and  $v_d=v_{o,VD}$  [Eq. (33)]. Both of these peak forces are assumed to occur during uplift of the pier and immediately following impact of the pier leg with the maximum impact velocity ( $v_{o,VD}$ ).

## Conclusions

The unidirectional and bidirectional kinematic and hysteretic properties of controlled rocking, four-legged steel truss piers have been investigated. Key variables for the cyclic hysteretic behavior of controlled rocking piers have been identified considering bidirectional horizontal response, and analytical expressions have been developed for their calculation. Results of nonlinear static pushover analysis are presented and compared with results obtained from these analytically derived expressions and shown to be in good agreement. A simplified method of analysis was proposed for prediction of maximum pier displacements. Design rules were established to determine maximum displacement demands and to achieve capacity protection of the pier. The design rules account for three components of ground excitation and dynamic effects caused by impacting and uplifting during the rocking response. It was proposed that unidirectional hysteretic properties are used for prediction of displacements since these properties would provide a lower bound on the pier's force and energy-dissipating capacity, thus providing an upper bound on prediction of the maximum displacement. On the other hand, bidirectional hysteretic behavior is considered for prediction of maximum forces to provide an upper bound and conservative estimate of the force response. This could be considered a type of bounding analysis for design. Nonlinear dynamic response history analyses were performed, and results have shown the design rules to conservatively predict response with respect to the mean response, except that results were slightly unconservative when using the 100-40 directional combination rule for prediction of displacement response (bidirectional pier displacement and uplifting displacement). Finally, the use of fluid VD's as the passive control devices in the controlled rocking system was discussed. Application of the simplified analysis method and design rules was established for the use of fluid VD's. Note that the analytical portion of this study included earthquake ground motions that did not contain characteristics typical of near-field seismic events. Seismic response of rocking structures that have significant nonlinear behavior may be influenced by the low-frequency pulses in the near field.

## Acknowledgments

This research was supported in part by the Federal Highway Administration under Contract No. DTFH61-98-C-00094 to the Multidisciplinary Center for Earthquake Engineering Research. However, any opinions, findings, conclusions, and recommendations presented in this paper are those of the writers and do not necessarily reflect the views of the sponsors.

## References

- AISC. (2005). *Seismic provisions for structural steel buildings*, Chicago.
- ATC/MCEER. (2004). "Recommended LRFD guidelines for the seismic design of highway bridges. Part I: Specifications." *NCHRP 12-49*, ATC/MCEER Joint Venture, ATC/MCEER, Buffalo, N.Y.
- Constantinou, M. C., Soong, T. T., and Dargush, G. F. (1998). *Passive energy dissipation systems for structural design and retrofit*, Monograph Series No. 1, Multidisciplinary Center for Earthquake Engineering Research, Univ. at Buffalo, The State Univ. of New York at Buffalo, Buffalo, N.Y.
- Dowdell, D., and Hamersley, B. (2001). "Lions' Gate Bridge North Approach: Seismic retrofit." *Behaviour Steel Structures in Seismic Areas: Proc., 3rd Int. Conf.: STESSA 2000*, Balkema, Rotterdam, The Netherlands, 319–326.
- FEMA. (2004). "NEHRP recommended provisions for seismic regulations for new buildings and other structures." *FEMA 450*, Building Seismic Safety Council for the FEMA, Washington, D.C.
- Housner, G. (1963). "The behavior of inverted pendulum structures during earthquakes." *Bull. Seismol. Soc. Am.*, 53(2), 403–417.
- Housner, G. (1990). "The governor's board of inquiry on the 1989 Loma Prieta earthquake." *Competing against time*, Office of Planning and Research, Sacramento, Calif.
- Ingham, T., Rodriguez, S., Nadar, M., Taucer, F., and Seim, C. (1997). "Seismic retrofit of the Golden Gate Bridge." *Proc., National Seismic Conf. on Bridges and Highways: Progress in Research and Practice*, FHWA, Washington, D.C.
- Jones, M., Holloway, L., Toan, V., and Hinman, J. (1997). "Seismic retrofit of the 1927 Carquinez Bridge by a displacement capacity approach." *Proc., 2nd National Seismic Conf. on Bridges and Highways: Progress in Research and Practice*, FHWA, Washington, D.C.
- Kelley, J., and Tsztoo, D. (1977). "Earthquake simulation testing of a stepping frame with energy-absorbing devices." *Rep. No. EERC 77-17*, Earthquake Engineering Research Center, College of Engineering, Univ. of California, Berkeley, Berkeley, Calif.
- Lee, K., and Bruneau, M. (2004). "Seismic vulnerability evaluation of axially loaded steel built-up laced members." *Technical Rep. No. MCEER-04-0007*, Multidisciplinary Center for Earthquake Engineering Research, State Univ. of New York at Buffalo, Buffalo, N.Y.
- Mander, J., and Cheng, C. (1997). "Seismic resistance of bridge piers based on damage avoidance design." *Technical Rep. No. NCEER-97-0014*, National Center for Earthquake Engineering Research, The State Univ. of New York at Buffalo, Buffalo, N.Y.
- Marriott, D., Palermo, A., and Pampanin, S. (2006). "Quasi-static and pseudo-dynamic testing of damage-resistant bridge piers with hybrid connections." *Proc., 1st ECEES*, Balkema, Rotterdam, The Netherlands.
- Meek, J. W. (1975). "Effects of foundation tipping on dynamic response." *J. Struct. Div.*, 101(ST7), 1297–1311.
- Midorikawa, M., Azuhata, T., Ishihara, T., and Wada, A. (2003). "Shaking table tests on rocking structural systems installed yielding base plates in steel frames." *Behaviour of Steel Structures in Seismic Areas, STESSA 2003*, Balkema, Rotterdam, The Netherlands, 449–454.
- Palermo, A., Pampanin, S., and Calvi, G. M. (2005). "Concept and development of hybrid solutions for seismic resistant bridge systems." *J. Earthquake Eng.*, 9(6), 899–921.
- Pollino, M., and Bruneau, M. (2007). "Seismic retrofit of bridge steel truss piers using a controlled rocking approach." *J. Bridge Eng.*, 12(5), 600–610.
- Pollino, M., and Bruneau, M. (2008). "Analytical and experimental investigation of a controlled rocking approach for seismic protection of bridge steel truss piers." *Technical Rep. No. MCEER-08-0003*, Multidisciplinary Center for Earthquake Engineering Research, The State Univ. of New York at Buffalo, Buffalo, N.Y.
- Priestley, M. J. N., Evison, R. J., and Carr, A. J. (1978). "Seismic response of structures free to rock on their foundations." *Bulletin of the*

- New Zealand National Society for Earthquake Engineering*, Vol. 11, No. 3, New Zealand.
- Priestley, M. J. N., Seible, F., and Calvi, G. M. (1996). *Seismic design and retrofit of bridges*, Wiley, New York.
- Prucz, Z., Conway, W. B., Schade, J. E., and Ouyang, Y. (1997). "Seismic retrofit concepts and details for long-span steel bridges." *Proc., 2nd National Seismic Conf. on Bridges and Highways: Progress in Research and Practice*, FHWA, Washington, D.C.
- Psycharis, I. N. (1982). "Dynamic behavior of rocking structures allowed to uplift." Ph.D. dissertation, California Institute of Technology, Pasadena, Calif.
- Toranzo, L. A., Restrepo, J. I., Mander, J. B., and Carr, A. J. (2009). "Shake-table tests of confined-masonry rocking walls with supplementary hysteretic damping." *J. Earthquake Eng.*, 13(6), 882–898.
- Wen, Y. K. (1976). "Method for random vibration of hysteretic systems." *J. Engrg. Mech. Div.*, 102(EM2), 249–263.
- Wilson, E. (2000). *Three dimensional static and dynamic analysis of structures*, Computers and Structures, Inc., Berkeley, Calif.